Time-Domain Simulations of the Nonlinear Maxwell Equations Using Operator-Exponential Methods

Martin Pototschnig, Jens Niegemann, Lasha Tkeshelashvili, and Kurt Busch, *Member*

***Abstract*—In this paper, we propose a Krylov-subspace-based operator-exponential method for time-domain simulations of the Maxwell equations with general nonlinear polarizations. This includes (classical) $\chi^{(2)}$- or $\chi^{(3)}$- nonlinearities and/or nonlinear coupled system dynamics. As an illustration, we compare the performance of our approach to certain well-known methods for the case of pulse self-steepening in a material with negative Kerr-nonlinearity. For this system, we also develop an appropriate analytical reference solution. In addition, we demonstrate that our approach allows to treat the complex nonlinear dynamics of various physical systems (classical and/or quantum) coupled to electromagnetic fields.**

***Index Terms*—Finite-difference time-domain (FDTD) methods, numerical analysis, optical Kerr effect.**

I. Introduction

FOR complex optical and photonic systems [1], numerical methods are of particular importance since only a very limited number of (mostly 1-D) problems are amenable to analytical or semi-analytical (variational, etc.) techniques. Therefore, the development of efficient numerical approaches lies at the heart of progress of photonics and is the subject of intense research efforts in the engineering, theoretical physics, and applied mathematics communities. Currently, the finite element method (FEM) [2] and the finite-difference time-domain (FDTD) approach [3] represent the well-documented standards for simulations of the Maxwell equations in frequency and time domain, respectively, that are continuously improved and refined.

The unavailability of the superposition principle mandates that the Maxwell equations for materials with nonlinear response properties have to be, in general, investigated within the framework of a time-domain approach. Unfortunately, the FDTD technique, which relies on finite-difference discretizations of the Maxwell equations on staggered grids [3], is only conditionally stable and great care has to be taken in order to minimize detrimental effects originating from spurious numerical dispersion. Nevertheless, the FDTD community has developed a multitude of techniques for dealing with various types of optical nonlinearities and we refer to [3] and [4] for an overview. These approaches avoid certain simplifying assumptions that lead to conventional approximations such as the asymptotic and paraxial-propagation analyses within nonlinear Schrödinger equation techniques [5] and the beam propagation method [6]. However, relative to these latter methods and not least owing to its limited time-stepping capabilities, nonlinear FDTD is certainly very computationally intensive.

In order to improve the time-integration aspect, several unconditionally stable methods based on operator exponentials have recently been suggested for the *linear* Maxwell equations [3], [7]. In particular, in [7], some of us have introduced a general-purpose Krylov-subspace-based operator-exponential technique and have compared this method to FDTD and other operator-exponential-based schemes. For many practical applications, it is highly desirable to extend these schemes to general *nonlinear* problems. First, many optical materials of interest exhibit sizeable nonlinear response which very often enters the Maxwell equations through (classical) nonlinear polarization terms such as those described via second- and third-order nonlinearities that are, respectively, described by the third- and fourth-rank susceptibility tensors, $\chi^{(2)}$ and $\chi^{(3)}$. Second, in many realistic cases—notably in strongly interacting and/or scattering nanophotonic systems—the coupling between electromagnetic waves and other physical systems cannot be described by linear and/or nonlinear susceptibilities that are obtained by "integrating out" the underlying materials' degrees of freedom. The point is that the coupling terms in the equations of motion of the combined system are nonlinear and the dynamics of the subsystems have to be treated on an equal footing in the form of coupled dynamical systems. In this work, we illustrate our approach of solving the general nonlinear Maxwell equations in the sense discussed above.

More precisely, in this paper, we extend the Krylov-subspace-based exponential integrators method of [7] to the concrete example of an instantaneous Kerr nonlinearity. The methods' extension to second-order and/or dispersive classical nonlinearities may be realized in a completely analogous manner. Furthermore, we also comment on and provide an outlook to the treatment of coupled systems dynamics. The primary strategy is to solve the linear part of the resulting set of differential equations with uncompromisingly high precision and then to evaluate the nonlinear part by standard (high-order) schemes. The excellent time-integration properties of the linear Krylov-subspace-based exponential integrator guarantees an

Manuscript received July 25, 2007; revised October 07, 2008. Current version published March 20, 2009. This work was supported by the Center for Functional Nanostructures (CFN) of the Deutsche Forschungsgemeinschaft (DFG) at the Universität Karlsruhe (TH) within project A1.2. The work of L. Tkeshelashvili and K. Busch was also supported by the DFG within priority program SPP 1113 under grant Bu 1107/6-1. In addition, the work of L. Tkeshelashvili was supported by USA CRDF Grant GEP2-2848-TB-06.

M. Pototschnig was with the Institut für Theoretische Festkörperphysik, Universität Karlsruhe, 76128 Karlsruhe, Germany. He is now with the Laboratory of Physical Chemistry (LPC), ETH Zürich, 8093 Zürich, Switzerland.

J. Niegemann, L. Tkeshelashvili, and K. Busch are with the Institut für Theoretische Festkörperphysik, Universität Karlsruhe, 76128 Karlsruhe, Germany (e-mail: kurt@tfp.uni-karlsruhe.de).

Color versions of one or more of the figures in this paper are available online at http://ieeexplore.ieee.org.

Digital Object Identifier 10.1109/TAP.2008.2011181

efficient treatment of highly oscillatory problems that often occur when considering the propagation of optical pulses. We would like to emphasize that—independent of the concrete method that underlies the linear and nonlinear solvers—such a strategy allows one to obtain realistic descriptions for the systems discussed above. For instance, in nonlinear wave-mixing phenomena, the accurate treatment of the waves' phases over long time scales is of paramount importance. If, however, the underlying linear solver is prone to numerical dispersion, the design of corresponding experiments or the interpretation of measurements become problematic.

This paper is organized as follows. In Section II, we introduce the general framework of two fourth-order-in-time nonlinear integrators that employ the Krylov-subspace operator-exponential approach of [7] as the associated linear solver. In Section III, we then report on the results of our comparative performance and accuracy analyses of these operator-exponential-based integrators, a standard (second-order) FDTD approach and a fourth-order Runge–Kutta integrator. In order to assess the accuracy of all methods, we develop in the Appendix—to the best of our knowledge for the first time—an analytic reference solution for the case of the 1-D Maxwell equations in the presence of Kerr-nonlinear materials. Finally, in Section IV, we summarize our findings and provide an outlook for future developments.

II. Exponential Integrators

We consider two distinct approaches to introduce exponentials into integrators for an arbitrary system of coupled first-order differential equations (SDE) such as that which emerges when spatially discretizing the general nonlinear Maxwell equations. For an overview of several other related approaches, we refer to [8].

The first method relies on certain (numerically feasible) approximations of the SDE's Jacobian, for instance, its entire linear part. Then, the remaining nonlinear part of the SDE is subjected to a standard integrator. We refer to this strategy as the L-NL method. The other approach employs, at each time step, the full Jacobian of the SDE and treats the residual (and nonlinear) part with a standard integrator. Below, we refer to this strategy as the J-R method. In both cases, the governing SDE must be rearranged into the general form of a Schrödinger-like equation

$$\frac{\partial}{\partial t}\Psi = \mathcal{H}\Psi + \mathcal{N}(\Psi, t). \tag{1}$$

Here, $\Psi \equiv \Psi(t)$ is the (generally very large) vector of unknown functions that has to be obtained via the time stepping of (1) from an initial condition $\Psi_0 \equiv \Psi(t_0)$ at time t_0. The operator $\mathcal{H}$ represents that part of the SDE that should be stepped via the (very accurate linear) exponential integrator and $\mathcal{N}(\Psi)$ represents the (nonlinear) part that is stepped with a (sufficiently accurate) standard method.

Although such a rearrangement of the underlying SDE might not always be possible, it is certainly doable for the Maxwell equations in almost all cases of interest. To be specific, we will carry out our subsequent analysis for the case of spatially structured, isotropic, and dispersionless Kerr-nonlinear materials. From this illustration, the treatment of other cases can be inferred in a straightforward manner. In addition, we will comment on the Maxwell–Bloch equations in Section IV.

In view of the above discussion, we write the time-dependent Maxwell equations for a Kerr-nonlinear medium as

$$\begin{aligned}\frac{\partial}{\partial t}\vec{D}(\vec{r},t) &= +\nabla\times\vec{H}(\vec{r},t)\\ \frac{\partial}{\partial t}\vec{B}(\vec{r},t) &= -\nabla\times\vec{E}(\vec{r},t)\end{aligned} \tag{2}$$

together with the constitutive relations

$$\vec{D}(\vec{r},t) = \epsilon_0\left(\epsilon(\vec{r}) + \chi^{(3)}(\vec{r})\left|\vec{E}(\vec{r},t)\right|^2\right)\vec{E}(\vec{r},t) \tag{3}$$

$$\vec{B}(\vec{r},t) = \mu_0\mu(\vec{r})\vec{H}(\vec{r},t). \tag{4}$$

The system is characterized through its linear relative dielectric permittivity $\epsilon(\vec{r})$, its linear relative magnetic permeability $\mu(\vec{r})$, and its nonlinear Kerr susceptibility $\chi^{(3)}(\vec{r})$. We would like to emphasize that the usage of (3) implies that the general constitutive relation $\vec{D}(\vec{E})$ has been approximated by a Taylor series in the electric field $\vec{E}$ [9]. In turn, this implies that the second term on the right-hand side of (3) is significantly smaller than the first term.

We now proceed to nondimensional field quantities via rescaling the electric field $\vec{E}$ and the displacement field $\vec{D}$ by the free-space permittivity ϵ_0. Similarly, we rescale the magnetic field $\vec{H}$ and the magnetic induction $\vec{B}$ by the free-space permeability μ_0. This rescaling implies that the vacuum speed of light is $c_0 = 1$. Upon introducing a spatial unit of length l and measuring time in units of l/c_0, we finally arrive at

$$\frac{\partial}{\partial t}\vec{E}(t) = \mathcal{C}(\vec{E})\nabla\times\vec{H}(t) - \vec{j}_{\rm el} \tag{5}$$

$$\frac{\partial}{\partial t}\vec{H}(t) = -\frac{1}{\mu}\nabla\times\vec{E}(t) - \vec{j}_{\rm mag}. \tag{6}$$

Here, in the interest of a compact notation, we have suppressed—and will continue to do so for the remainder of this paper—all explicit dependencies on the spatial argument $\vec{r}$.

In (5), we have introduced a matrix $\mathcal{C}(\vec{E})$ that relates the time derivatives of the displacement field $\vec{D}$ and the electric field $\vec{E}$ according to

$$\frac{\partial}{\partial t}\vec{E} = \mathcal{C}(\vec{E})\frac{\partial}{\partial t}\vec{D}. \tag{7}$$

In fact, although the relation between the electric field and the displacement field (3) is isotropic, the corresponding relation between the temporal derivatives is not. Starting form (3) in dimensionless quantities and differentiating with respect to time yields

$$\frac{\partial}{\partial t}\vec{D}(t) = \left[\epsilon_{\rm nl}\mathbf{1} + 2\chi^{(3)}\mathcal{A}\right]\frac{\partial}{\partial t}\vec{E}(t) \tag{8}$$

where we have introduced the (3×3)-unit matrix $\mathbf{1}$ along with the abbreviations $\epsilon_{\rm nl} = \epsilon + \chi^{(3)}|\vec{E}|^2$ and

$$\mathcal{A} = \begin{pmatrix} E_1^2 & E_1E_2 & E_1E_3\\ E_1E_2 & E_2^2 & E_2E_3\\ E_1E_3 & E_2E_3 & E_3^2\end{pmatrix}. \tag{9}$$

By inverting this relation, we obtain $\mathcal{C}(\vec{E})$ as

$$\mathcal{C}(\vec{E}) = \frac{\left(\epsilon^2 + 4\chi^{(3)}\epsilon|\vec{E}|^2 + 3\left(\chi^{(3)}\right)^2|\vec{E}|^4\right)\mathbf{1} - 2\chi^{(3)}\epsilon_{\rm nl}\mathcal{A}}{(\epsilon_{\rm nl})^2\left(\epsilon + 3\chi^{(3)}|\vec{E}|^2\right)} \tag{10}$$

as long as $(\epsilon_{\rm nl})^2(\epsilon+3\chi^{(3)}|\vec{E}|^2)\neq 0$. This condition is fulfilled for $|3\chi^{(3)}|\vec{E}|^2|<|\epsilon|$ and, therefore, applies to the case of a valid description via the truncated Taylor series of $\vec{D}(\vec{E})$ as discussed above.

Furthermore, in (5) and (6), we have introduced losses via the (spatially varying) currents $\vec{j}_{\rm el}=\sigma_{\rm el}\vec{E}(t)$ and $\vec{j}_{\rm mag}=\sigma_{\rm mag}\vec{H}(t)$. The electric conductivity $\sigma_{\rm el}$ allows to incorporate physical (ohmic) losses. Both the electric conductivity $\sigma_{\rm el}$ and the magnetic conductivity $\sigma_{\rm mag}$ allow the realization of open boundary conditions via (unphysical) perfectly matched layers [3].

Upon introducing the supervector

$$\Psi(t)=\begin{pmatrix}\vec{E}(t)\\ \vec{H}(t)\end{pmatrix} \tag{11}$$

we can now realize a splitting of the SDE, (5) and (6), into linear and nonlinear parts as required by the L-NL method

$$\mathcal{H}=\begin{pmatrix}-\sigma_{\rm el} & \frac{1}{\epsilon(\vec{r})}\nabla\times\\ -\frac{1}{\mu(\vec{r})}\nabla\times & -\sigma_{\rm mag}\end{pmatrix} \tag{12}$$

$$\mathcal{N}(\Psi)=\begin{pmatrix}\left(\mathcal{C}(\vec{E})-\frac{1}{\epsilon(\vec{r})}\right)\nabla\times\vec{H(t)}\\ 0\end{pmatrix}. \tag{13}$$

A similar splitting of (5) and (6) that is consistent with the J-R method is only notationally more involved. To do so, we introduce the scalar $\epsilon_{\rm nl,0}=\epsilon+\chi^{(3)}|\vec{E}(t_0)|^2$, the vectors $\vec{E}_0=\vec{E}(t_0)$, $\vec{H}_0=\vec{H}(t_0)$, and the matrix

$$\mathcal{T}_0=\left(\frac{\partial\mathcal{C}}{\partial E_1}(\vec{E}_0)\quad\frac{\partial\mathcal{C}}{\partial E_2}(\vec{E}_0)\quad\frac{\partial\mathcal{C}}{\partial E_3}(\vec{E}_0)\right)\nabla\times\vec{H}_0. \tag{14}$$

This matrix $\mathcal{T}_0$ consists of column vectors that are obtained by multiplying the matrices $\partial\mathcal{C}/\partial E_j$ $(j=1,2,3)$ with the vector $\nabla\times\vec{H}_0$. Here, we want to recall that all these quantities do depend on the spatial coordinate $\vec{r}$. With these abbreviations, we may, at any time t_0 that is required in the time-stepping, split (5) and (6) into Jacobian and residual according to

$$\mathcal{H}=\begin{pmatrix}-\sigma_{\rm el}+\mathcal{T}_0 & \mathcal{C}(\vec{E}_0)\nabla\times\\ -\frac{1}{\mu}\nabla\times & -\sigma_{\rm mag}\end{pmatrix} \tag{15}$$

$$\mathcal{N}(\Psi)=\begin{pmatrix}-\mathcal{T}_0\vec{E}(t)+\left(\mathcal{C}\left(\vec{E}(t)\right)-\mathcal{C}(\vec{E}_0)\right)\nabla\times\vec{H}(t)\\ 0\end{pmatrix}. \tag{16}$$

The splitting of the Maxwell equations (5) and (6) into linear and nonlinear parts (12) and (13) yields an operator $\mathcal{H}$ that is independent of the electric and magnetic fields. In contrast, the splitting into Jacobian and residual (15) and (16) results in an operator $\mathcal{H}$ that has to be evaluated anew at every time step t_0.

Direct calculation of $\partial\mathcal{C}/\partial E_j$ yields

$$\frac{\partial C}{\partial E_j}(\vec{E}_0)=\frac{\alpha_j}{\left[(\epsilon_{\rm nl,0})^2\left(\epsilon+3\chi^{(3)}|\vec{E}_0|^2\right)\right]^2} \tag{17}$$

where the matrix α_j reads as

$$\begin{aligned}\alpha_j=&2\chi^{(3)}\epsilon_{\rm nl,0}E_j\left[\left(-\epsilon^3-7\chi^{(3)}\epsilon^2|\vec{E}_0|^2\right.\right.\\ &\left.-15\left(\chi^{(3)}\right)^2\epsilon|\vec{E}_0|^4-9\left(\chi^{(3)}\right)^3|\vec{E}_0|^6\right)\mathbf{1}\\ &+2\chi^{(3)}\epsilon_{\rm nl,0}(6\epsilon_{\rm nl,0}-2\epsilon)\mathcal{A}\Big]\\ &-2\chi^{(3)}\epsilon_{\rm nl,0}\left[(\epsilon_{\rm nl,0})^2(3\epsilon_{\rm nl,0}-2\epsilon)\frac{\partial\mathcal{A}}{\partial E_j}\right].\end{aligned} \tag{18}$$

We now proceed to spatially discretize the entire system. The simplest method would employ a standard Yee-grid [3], but more sophisticated discretizations via appropriate finite elements [2] or wavelets [10] are conceivable. Independent of the nature of the actual spatial discretization procedure, we generally obtain a very large vector $\Psi(t)$ and, correspondingly, very large but sparse linear and nonlinear operators $\mathcal{H}$ and $\mathcal{N}$, respectively.

A. Lawson Exponential Integrators

One particular class of exponential integrators consists of the so-called Lawson exponential integrators [11]. They are often referred to as integrating factor methods.

The central idea of these methods is to employ a new variable $A=e^{-t\mathcal{H}}\Psi$ that transfers the SDE (1) into

$$\frac{\partial A}{\partial t}=\mathcal{F}(A,t)=e^{-t\mathcal{H}}\mathcal{N}(e^{+t\mathcal{H}}A). \tag{19}$$

The primary advantage of this transformation is that the linear part is completely eliminated. As a result, we can apply explicit schemes such as the explicit Euler method to (19)

$$A(t_{n+1})=A(t_n)+\Delta t\mathcal{F}\left(A(t_n),t_n\right) \tag{20}$$

where we have introduced the (fixed) time step $\Delta t:=t_{n+1}-t_n$ between times t_{n+1} and t_n. Upon transforming back to the old variables, we arrive at the so-called Lawson–Euler scheme

$$\Psi(t_{n+1})=e^{\mathcal{H}\Delta t}\Psi(t_n)+\Delta te^{\mathcal{H}\Delta t}\mathcal{N}\left(\Psi(t_n)\right). \tag{21}$$

We would like to emphasize that, in principle, we could choose the splitting between the linear and the nonlinear parts arbitrarily, i.e., either use the L-NL or the J-R method. However, for actual implementations of most schemes based on the Lawson transformation, the L-NL method is significantly more efficient than the J-R method. For our subsequent analyses, we have implemented a so-called Lawson4 scheme, which is based on the classical fourth-order Runge–Kutta method

$$\begin{aligned}Y_1&=\Psi(t_{n-1})\\ Y_2&=\frac{\Delta t}{2}e^{\Delta t\mathcal{H}}\mathcal{N}(Y_1,t_{n-1})+e^{\frac{\Delta t\mathcal{H}}{2}}Y_1\\ Y_3&=\frac{\Delta t}{2}\mathcal{N}\left(Y_2,t_{n-\frac{1}{2}}\right)+e^{\frac{\Delta t\mathcal{H}}{2}}Y_1\\ Y_4&=\Delta te^{\frac{\Delta t\mathcal{H}}{2}}\mathcal{N}\left(Y_3,t_{n-\frac{1}{2}}\right)+e^{\Delta t\mathcal{H}}Y_1\\ \Psi(t_n)&=\frac{\Delta t}{6}\left[e^{\Delta t\mathcal{H}}\mathcal{N}(Y_1,t_{n-1})+2e^{\frac{\Delta t\mathcal{H}}{2}}\mathcal{N}\left(Y_2,t_{n-\frac{1}{2}}\right)\right.\\ &\qquad\left.+2e^{\frac{\Delta t\mathcal{H}}{2}}\mathcal{N}\left(Y_3,t_{n-\frac{1}{2}}\right)+\mathcal{N}(Y_4,t_n)\right]\\ &\quad+e^{\Delta t\mathcal{H}}Y_1.\end{aligned} \tag{22}$$

Here, we have introduced $t_{n-(1/2)}:=t_{n-1}+\Delta t/2$. In order to guarantee that the entire Lawson4 integrator (22) is fourth order in time, we evaluate the matrix exponentials through Krylov-subspace techniques [7], [12]–[14] with a Krylov-subspace dimension of 6. Since the operator

exponential has to be applied to $\Psi(t_{n-1})$, $\mathcal{N}(Y_1, t_{n-1})$, $\mathcal{N}(Y_2, t_{n-(1/2)})$, and $\mathcal{N}(Y_3, t_{n-(1/2)})$, a total of four Krylov subspaces are required for a single time step. However, the calculation of $\exp(\Delta t\mathcal{H}/2)\Psi(t_{n-1})$ and $\exp(\Delta t\mathcal{H})\Psi(t_{n-1})$ can be performed in the same Krylov subspace by squaring the transformed (small 6×6) matrix resulting from $\exp(\Delta t\mathcal{H}/2)\Psi(t_{n-1})$. In principle, this scheme could be further optimized by evaluating the nonlinear terms within the same Krylov subspace. Such an approximation might, however, reduce the order of the method and further research needs to be done.

Higher order schemes can be realized through appropriate higher order Runge–Kutta methods together with a corresponding increase of the Krylov-subspace dimension. However, this would significantly increase the memory usage relative to standard second-order-in-time FDTD. Therefore, our above choice represents a suitable compromise for applications to many nanophotonic systems.

B. Rosenbrock–Wanner Exponential Integrators

Another class of exponential integrators is based on implicit methods of Rosenbrock–Wanner type. These integrators are generally less intuitive than the Lawson integrators but can offer better performance characteristics. As an illustration of this approach, we first consider the following initial value problem:

$$\frac{\partial y}{\partial t} = f(y), \qquad y(0) = y_0 \tag{23}$$

with an arbitrary function $f(y)$ and apply the A-stable implicit Euler scheme. As a result, we obtain

$$\frac{y_{n+1} - y_n}{\Delta t} = f(y_{n+1}). \tag{24}$$

In general, this set of equations is nonlinear and, therefore, it is difficult to solve for the desired solution y_{n+1} at time t_{n+1}. The central idea of all Rosenbrock–Wanner methods is to linearize these equations according to

$$y_{n+1} = y_n + \Delta t f(y_n) + \Delta t \frac{\partial f}{\partial y}(y_n)(y_{n+1} - y_n). \tag{25}$$

The resulting set of linear equations is easily solved by means of standard methods. Moreover, the above procedure can be generalized to multistep methods

$$\begin{aligned} k_i &= \varphi_{\mathrm{RW}}(\gamma\Delta t A)\left(f(u_i) + \Delta t A \sum_{j=1}^{i-1} \gamma_{ij} k_j\right), \qquad i = 1, \ldots, s \\ u_i &= y_n + \Delta t \sum_{j=1}^{i-1} \alpha_{ij} k_j \\ y_{n+1} &= y_n + \Delta t \sum_{i=1}^{s} b_i k_i \end{aligned} \tag{26}$$

where s is the number of steps and α_{ij}, b_i, γ_{ij}, and γ denote free parameters. The matrix $A \equiv f'(y_n)$ represents the Jacobian resulting from the linearization and $\varphi_{\mathrm{RW}}(A) = \mathrm{I}/(\mathrm{I} - A)$ is the characteristic of the implicit Rosenbrock–Wanner methods. We would like to notice that the above scheme reduces to explicit Runge–Kutta methods if we—instead of the Rosenbruck–Wanner choice—were to use $\gamma_{ij} = 0$ and replace φ_{RW} with $\varphi_{\mathrm{RK}} = \mathrm{I}$.

At this stage, exponential integrators may be employed to solve the linear part exactly (or with sufficiently high accuracy) instead of using the simple finite-difference approach in (24). For instance, consider the linear case

$$\frac{\partial y}{\partial t} = f(y) = Ay + b \tag{27}$$

with constant inhomogeneity b and matrix A. In this case, the implicit Euler method gives

$$\begin{aligned} (\mathbf{I} - \Delta t A)k_1 &= f(u_1) \\ u_1 &= y_n \\ y_{n+1} &= y_n + \Delta t k_1 \end{aligned} \tag{28}$$

where $s = 1$, $k_1 = (y_{n+1} - y_n)/\Delta t$, and $b_1 = 1$. In contrast, the exact solution of (27) can be found via the variation-of-constants formula

$$\begin{aligned} y_{n+1} &= e^{\Delta t A} y_n + \int_{t_n}^{t_{n+1}} e^{(t_{n+1} - t)A} b \mathrm{d}t \\ &= y_n + \Delta t \varphi(\Delta t A) f(y_n). \end{aligned} \tag{29}$$

Here, $\varphi(A) := (e^A - \mathrm{I})/A$ denotes a function that is closely related to the exponential function as seen from the corresponding power series $\varphi(A) = \sum_{k=0}^{\infty} A^k/(k+1)!$. In fact, the Krylov-subspace technique for evaluating operator exponential can easily be adapted to evaluate $\varphi(A)$. It is also interesting to compare this $\varphi(A)$ with the $\varphi_{\mathrm{RW}}(A)$ that originates from the finite-difference discretization of the time derivative.

Based on the above reasoning, Hochbruck *et al.* [15] have suggested the following fourth-order method

$$\begin{aligned} k_1 &= \varphi\left(\frac{1}{2}\Delta t A\right) f(y_n) \\ k_2 &= \varphi(\Delta t A) f(y_n) \\ w_3 &= \frac{3}{8}(k_1 + k_2) \\ u_3 &= y_n + \Delta t w_3 \\ d_3 &= f(u_3) - f(y_n) - \Delta t A w_3 \\ k_3 &= \varphi\left(\frac{1}{2}\Delta t A\right) d_3 \\ y_{n+1} &= y_n + \Delta t \left(k_2 + \frac{16}{27} k_3\right). \end{aligned} \tag{30}$$

Here, we have defined the auxiliary vectors d_i as

$$d_i = f(u_i) - f(y_n) - \Delta t A \sum_{j=1}^{s} \alpha_{ij} k_j. \tag{31}$$

We have implemented this scheme for use with our Krylov-subspace-based evaluation of the matrix function $\varphi(A)$ and will subsequently refer to it as the Hochbruck4 scheme.

The Rosenbruck–Wanner techniques in general and the Hochbruck4 scheme in particular rely on the exact Jacobian of the SDE at each time step. If an approximate Jacobian would be employed (such as is the case for the Lawson integrators),

the method immediately loses all its attractive features and becomes only first-order accurate. However, for a single time step, the Hochbruck4 scheme requires only two Krylov subspaces, since $\varphi((1/2)\Delta t\ A)f(y_n)$ and $\varphi(\Delta t\ A)f(y_n)$ can both be computed in the same subspace. In addition, we can reduce the computational effort even further by using a smaller Krylov-subspace dimension to approximate $\varphi((1/2)\Delta t\ A)d_3$. This approximation utilizes the fact that the norm of d_3 is much smaller than the norm of $f(y_n)$ [15]. For the performance comparison of various solvers in Section III, we have operated the Hochbruck4 scheme with Krylov-subspace dimensions 6 and 3 for the evaluation of the first two φ-functions and the third φ-function, respectively. In total, we find that although the Hochbruck4 scheme leads to a substantial computational overhead that stems from the evaluation of the exact Jacobian at every time step, it does offer certain advantages that make it very competitive as a high-order solver for the nonlinear Maxwell equations (see Section III).

In the next section, we compare the performance of several integrators of the nonlinear Maxwell equations (2) for a uniform 1-D system with negative Kerr nonlinearity and Gaussian-pulse initial conditions. For this system, we have developed an analytical reference solution of the full nonlinear Maxwell equations. The corresponding details and notations can be found in the Appendix. This reference system features a self-steepening behavior of the propagating pulse that eventually leads to the formation of a shock where the wave breaks and the reference solution is no longer valid. Therefore, the total simulation time has been limited so as to avoid wave breaking to occur. Nevertheless, significant pulse deformations already set in well before so that this system represents a serious test for any nonlinear Maxwell solver.

III. Performance of the Integrators

When investigating the performance of any Maxwell solver, one has to bear in mind that a numerical solution has two general aspects: the time stepping and the spatial discretization. Within standard FDTD, the two are interrelated (leap-frogging and Yee-grid), whereas in the case of operator-exponential time integrators, the spatial discretization can, in principle, be chosen independently. In this work, we analyze our time integrator for nonlinear problems and, therefore, we chose the least problematic spatial dimension. Furthermore, to the best of our knowledge, analytic reference solution are only available for 1-D systems. Therefore, our restriction to 1-D problems will result in a rather conservative comparison of our operator-exponential approach with the well-established FDTD method regarding both efficiency and accuracy.

More precisely, in the Appendix, we have demonstrated that for a uniform 1-D system with negative Kerr nonlinearity, well-behaved initial condition $E(0,x) \in C^1(\mathbb{R})$, and sufficiently small times $t \in [0, T_{\max}]$, the unique analytic solution to the Maxwell equations (2) is

$$E(t,x) = E\left(0, x - \frac{1}{\sqrt{1+\frac{3\chi^{(3)}E(t,x)^2}{\epsilon}}}\frac{t}{\sqrt{\epsilon\mu}}\right)$$

$$H(t,x) = \sqrt{\frac{\epsilon}{\mu}} f\left(\frac{3\chi^{(3)}E(t,x)^2}{\epsilon}\right) E(t,x)$$

where the function $f(x)$ has been defined in (43) and (44). As an initial condition, we use a rescaled Gaussian pulse $E(0,x) = E_0 e^{-(x-x_0)^2/2\sigma}$ ($E_0 = 1$ and $\sigma = 5/\sqrt{2}$) centered at $x_0 = 25$. The values of the material parameters are $\epsilon = 1$, $\mu = 1$, and $\chi^{(3)} = -0.08$. This reference solution is determined up to machine precision within the time interval $[0, 15]$ using a fix-point iteration of (46).

Owing to the absence of system-inherent oscillations, this test problem does not fully utilize the potential of our exponential integrators. In fact, these exponential integrators are specifically geared towards multiple time scale and/or inherently oscillatory problems such as the Maxwell–Bloch equations [16] and many other coupled systems. On the other hand, this choice of test problem allows a fair comparison of several significantly different general purpose integrators of the Maxwell equations (2) such as standard FDTD, classical fourth-order Runge–Kutta, and the exponential integrators described in Section II. The problem here is that for high-frequency wave propagation FDTD quickly develops numerical dispersion when the time step is too large. Similarly, Runge–Kutta integrators typically do not fare well in oscillatory problems due to the (generally) stiff nature of the corresponding SDE. Therefore, we may regard the results below as a conservative estimate of the relative merits of these methods.

For all integrators, we spatially discretize (2) on an interval $[0, 100]$ using a (staggered) Yee-grid with 2001 and 2000 grid points for the E- and H-field, respectively. Within our nondimensional units [see discussion above, (5)], we can, for instance, choose the total system length to be 1 mm. Then, the system is discretized in steps of 500 nm and the total nondimensional simulation time $T = 15$ would correspond to a physical simulation time of about 50 picoseconds.

The spatial derivatives are approximated through eighth-order accurate stencils. However, we would like to note that the same accuracy is already achieved with sixth-order accurate stencils. In addition, for this particular problem, the actual choice of boundary conditions does not have any influence on the solution.

Finally, we define the relative error as $\|E - E_{\text{ref}}\|/\|E_{\text{ref}}\|$, where $\|E\| = \left(\sum_i E_i^2\right)^{1/2}$ is the Euklidean-norm of the discretized vector of the electric field $E = (E_1, \ldots, E_N)$ having N discretization points.

In Fig. 1, we display the results of our performance comparison of the various integrators alluded to above on an AMD Athlon64 3500+ processor. Instead of plotting the relative error versus actual time step Δt, we plot the relative error as a function of the actual computation time required to obtain the result. This takes into account that different integrators utilize different time steps and each individual time step may be computationally more or less involved so that only the total consumed central processing unit (CPU) time is a fair measure of the performance. In all cases, it has been carefully checked that the FDTD results do not compromise numerical dispersion which—in contrast to the Krylov-subspace solvers—is already present in any linear FDTD solver. The leveling off of the relative error for the Lawson4, classical Runge–Kutta, and Hochbruck4 schemes just above values around 10^{-10} is entirely due to the finite machine precision.

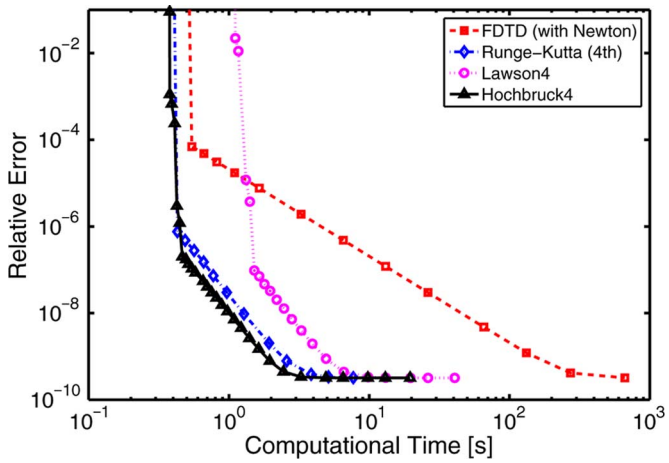

Fig. 1. Performance characteristics of various integrators of the nonlinear Maxwell equations for a uniform 1-D system with a (negative) Kerr nonlinearity. At time $t = 0$, a Gaussian pulse is launched. As time progresses, this system exhibits pulse steepening and, eventually, wave breaking occurs. The corresponding set of nonlinear Maxwell equations is amenable to an analytic solution, which serves as the reference for determining the relative errors. See text for further details.

For the standard-FDTD method, we have to solve a cubic equation for the electric field at each time step. This is done by applying two Newton iteration steps. One step is insufficient because in this case FDTD exhibits only first-order convergence. Conversely, more than two iteration steps only cost computational time without significantly improving the results. As expected, this standard FDTD solver exhibits a second-order behavior while the other solvers show a fourth-order characteristic. Also, as expected for this problem, the overhead incurred by the Lawson transformation leads to a better performance of the classical Runge–Kutta solver relative to the Lawson4 solver. Quite remarkably, the Hochbruck4 solver outperforms all other solvers. Owing to the specific nature of the test problem, the superiority over the classical Runge–Kutta solver is not too significant. As alluded to above, this may be quite different for problems involving multiple time scales (see also the discussion of the Maxwell–Bloch equations in Section IV). In contrast, the superiority of the Hochbruck4 solver over both, FDTD and Lawson4 integrators is rather significant. More precisely, in order to achieve the (machine-precision limited) minimal error, the Hochbruck4 solver requires roughly 1% and 20% of the CPU time of the standard FDTD solver and Lawson4 solver, respectively.

IV. Conclusion and Outlook

In conclusion, we have extended the Krylov-subspace-based exponential integrators method for linear problems [7] to the case of the general nonlinear Maxwell equations. The central idea of this approach is to solve the linear part of the SDE with high precision so that the nonlinear part can be treated via high-order standard methods. This feature is of particular importance since it allows one to efficiently treat stiff and highly oscillatory problems that are known to be difficult to handle by means of many standard solvers. Together with the performance comparison for a simple system with Kerr nonlinearity, this suggests that our approach has significant advantages compared to the FDTD method and the classical Runge–Kutta scheme. In particular, we anticipate that besides problems involving classical Kerr nonlinearities, the exponential integrators described in this paper will be particularly useful for the treatment of wave mixing phenomena in materials with second-order nonlinearities ($\chi^{(2)}$-nonlinearities).

Moreover, our scheme is flexible enough to incorporate various coupling effects of the electromagnetic fields with other physical systems as well. For instance, the semi-classical Maxwell–Bloch equations describe the radiation dynamics of an ensemble of two-level atoms. If a collection of identical atoms is located within a (compared to the cubic wavelength) small volume centered around $\vec{r}_0$, the corresponding SDE reads as

$$\begin{aligned}
\frac{\partial}{\partial t}\vec{E}(\vec{r},t) &= \frac{1}{\epsilon(\vec{r})}\nabla\times\vec{H}(\vec{r},t) \\
&\quad + \frac{n_{\mathrm{atom}}\vec{d}_r}{\epsilon(\vec{r})}\left(\omega_{21}\rho_2(\vec{r}_0,t) - \frac{1}{T_2}\rho_1(\vec{r}_0,t)\right) \\
\frac{\partial}{\partial t}\vec{H}(\vec{r},t) &= -\frac{1}{\mu(\vec{r})}\nabla\times\vec{E}(\vec{r},t), \\
\frac{\partial}{\partial t}\rho_1(\vec{r}_0,t) &= -\omega_{21}\rho_2(\vec{r}_0,t) - \frac{1}{T_2}\rho_1(\vec{r}_0,t) \\
\frac{\partial}{\partial t}\rho_2(\vec{r}_0,t) &= \omega_{21}\rho_1(\vec{r}_0,t) - \frac{1}{T_2}\rho_2(\vec{r}_0,t) \\
&\quad + \frac{2}{\hbar}\left(\vec{d}_r\cdot\vec{E}(\vec{r}=\vec{r}_0,t)\right)\rho_3(\vec{r}_0,t) \\
\frac{\partial}{\partial t}\rho_3(\vec{r}_0,t) &= -\frac{1}{T_1}\left(\rho_3(\vec{r}_0,t)-\rho_0\right) \\
&\quad - \frac{2}{\hbar}\left(\vec{d}_r\cdot\vec{E}(\vec{r}=\vec{r}_0,t)\right)\rho_2(\vec{r}_0,t).
\end{aligned} \tag{32}$$

Here, the density of atoms is denoted by n_{atom}. Furthermore, $\vec{d}_r$ and ω_{21} denote the atom's dipole matrix element (assumed to be real-valued) and transition frequency, respectively. The entries of the ensemble's density matrix ρ are denoted by $\rho_1 \equiv \mathrm{Re}(\rho_{12})$, $\rho_2 \equiv \mathrm{Im}(\rho_{12})$, and $\rho_3 \equiv \rho_{22} - \rho_{11}$. Besides radiative processes, the atomic inversion ρ_3 can decay via nonradiative processes (modeled through the nonradiative lifetime T_1) to its equilibrium value ρ_0. Similarly, the ensemble's in- and out-of-phase polarization components ρ_1 and ρ_2 can decay on a time scale T_2 via dephasing processes.

In a strongly scattering photonic environment, the linear dielectric permittivity $\epsilon(\vec{r})$ and (less common) the magnetic permeability $\mu(\vec{r})$ describe strong multiple scattering processes that can modify the propagation characteristics of the emitted radiation. In turn, this can lead to feedback (also called memory) effects where the atoms reabsorb and re-emit radiation and the usual Born and Markov approximations break down. This strongly non-Markovian behavior is encoded into the Maxwell–Bloch equations (32) through the nonlinear terms that couple the elements of the density matrix to the electric field. The ensemble's polarization terms then act as sources in the Maxwell equations. For typical values of the atomic transition frequency ω_{21} and dipole moment $\vec{d}_r$, emission processes are in the nanosecond range. In other words, at optical frequencies, the inversion ρ_3 varies on significantly larger time scales than the optical period. Therefore, the Maxwell–Bloch

equations represent a typical problem of coupled-systems dynamics where the capabilities of the exponential integrators such as efficiency, excellent long time stability, and accuracy that we have described in this paper are of relevance.

APPENDIX
A REFERENCE SOLUTION

In order to compare the efficiency of various integrators of the Maxwell equations, a suitable reference solution is required. For the present case of the *nonlinear* Maxwell equations, this is not an easy task. There exist a number of analytical solutions for certain nonlinear wave propagation problems (see, for instance, [17]–[19]). However, these solutions are solutions to equations, which themselves are approximations to the full nonlinear Maxwell equations. For instance, in [17] and [19], solutions to the (modified) nonlinear Schrödinger equation are developed, whereas [18] describes solutions to the wave equation in the presence of an intensity-dependent nonlinear refractive index but wave mixing processes are ignored. Therefore, in this appendix, we consider a simple 1-D problem, which lends itself to an analytical solution of the full nonlinear Maxwell equations. To the best of our knowledge, this analytical solution has not been reported before. However, we want to note that—different from our approach—this problem can also be treated using the methods of characteristics [20].

In the absence of sources and free charges, the Maxwell equations for uniform, isotropic Kerr-nonlinear dielectric media ($\epsilon \geq 1$ and $\mu \geq 1$) in one dimension are

$$\partial_t E = \frac{1}{\epsilon + 3\chi^{(3)}E^2}\partial_x H \tag{33}$$

$$\partial_t H = \frac{1}{\mu}\partial_x E \tag{34}$$

$$\partial_z D = 0 \tag{35}$$

$$\partial_y B = 0. \tag{36}$$

In these equations, the electric displacement D and the magnetic induction B are defined as

$$\begin{aligned} D &= \left(\epsilon + \chi^{(3)}E^2\right)E \\ B &= \mu H \end{aligned} \tag{37}$$

where $\chi^{(3)}$ denotes the Kerr coefficient of the material. For the purpose of obtaining an explicit reference solution with interesting physical behavior, we will in the following treat the case of a negative Kerr coefficient $\chi^{(3)} < 0$. Then, a pulse propagating in a homogeneous medium will experience self-steeping that eventually leads to the formation of a shock wave. In addition, we assume that the electromagnetic field evolves along the x-axis and that electric $E \equiv E_z$ and magnetic $H \equiv H_y$ fields are polarized along the z- and y-axis, respectively. Finally, we want to note that, as described in Section I, we have chosen rescaled units such that the speed of light is $c_0 \equiv 1$ and the linear material parameters ϵ and μ are dimensionless.

In order to facilitate a solution to (33)–(36), we make the following Ansatz:

$$\begin{aligned} E &= E(x,t) \\ H &= \sqrt{\frac{\epsilon}{\mu}} f\left(\frac{3\chi^{(3)}E(x,t)^2}{\epsilon}\right) E(x,t) \end{aligned}$$

with an analytic function $f(x)$ that, by construction, fulfills (35) and (36). With this Ansatz, we obtain from (33)

$$\partial_t E = \frac{1}{1+\xi}\frac{1}{\sqrt{\epsilon\mu}}\left[f(\xi) + f'(\xi)2\xi\right]\partial_x E \tag{38}$$

and from (34)

$$\left[f(\xi) + f'(\xi)2\xi\right]\partial_t E = \frac{1}{\sqrt{\epsilon\mu}}\partial_x E. \tag{39}$$

In the above expressions, $f'(\xi)$ denotes the derivative of the function $f(\xi)$ with respect to its argument, and we have abbreviated

$$\xi := \frac{3\chi^{(3)}E^2}{\epsilon}. \tag{40}$$

A nontrivial solution to (38) and (39) exists only when (38) and (39) are identical. This gives

$$\left[f(\xi) + f'(\xi)2\xi\right]^2 = (1+\xi) \tag{41}$$

or, equivalently

$$f(\xi) + f'(\xi)2\xi = \pm\sqrt{(1+\xi)}. \tag{42}$$

We observe that in the linear case (i.e., when $\xi = 0$), we have $f(0) = \pm 1$, corresponding to solutions that either travel to the left ($f(0) = +1$) or to the right ($f(0) = -1$). Owing to the symmetry of the problem, we concentrate below on the solution of a (nonlinear) wave moving to the right-hand side and, accordingly, choose $f(0) = -1$.

The differential equation (42) can be solved by utilizing a power series Ansatz

$$f(\xi) = \sum_{n=0}^{\infty} a_n \xi^n \tag{43}$$

where the coefficients a_n are

$$a_n = (-1)^n \frac{(2n-3)!!}{2^n(2n+1)n!}, \qquad n > 0, \qquad \text{and } a_0 = -1. \tag{44}$$

Here, $n!!$ denotes the product of all natural odd numbers k with $k \leq n$ (with the definition $n!! = 1$, for $n \leq 0$).

As a result, we obtain a single partial differential equation for the electric field $E(x,t)$

$$\partial_t E = \frac{-1}{\sqrt{1 + \frac{3\chi^{(3)}E^2}{\epsilon}}}\frac{1}{\sqrt{\epsilon\mu}}\partial_x E. \tag{45}$$

This equation has the implicit solution

$$E(x,t) = F\left(x - \frac{1}{\sqrt{1+\frac{3\chi^{(3)}E^2}{\epsilon}}}\frac{t}{\sqrt{\epsilon\mu}}\right) \tag{46}$$

where $F(E) \equiv F(E(x,t))$ may be any function with a continuous first derivative, i.e., $F \in C^1$.

In particular, for a Gaussian pulse with width σ as an initial condition, we obtain for $F(E)$

$$F = E_0 \exp\left(-\frac{1}{2\sigma^2}\left(x - \frac{1}{\sqrt{1+\frac{3\chi^{(3)}E^2}{\epsilon}}}\frac{t}{\sqrt{\epsilon\mu}}\right)^2\right). \tag{47}$$

To analyze the conditions for the existence of a solution of the implicit equation (46), we consider the Banach space $\mathcal{R} = (\mathbb{R}, |\cdot|)$ at constant time t and position x. While the position x may be an arbitrary real number, we will discuss below that it is useful to further restrict the time t to lie within a certain interval $t \in [0, T_{\max}]$. Then, Banach's fix-point theorem guarantees the existence of a solution of $F(E) = E$ [and, hence, of (46)] if the condition

$$\left|\frac{\partial F(E)}{\partial E}\right| \le C < 1 \tag{48}$$

is fulfilled for a certain constant $C < 1$. For the present situation of a negative Kerr coefficient $\chi^{(3)} < 0$, the explicit form of (46) for our reference solution suggests that during propagation, a self-steepening of the pulse will occur that eventually will lead to a "breaking" of the wave solution. This situation is similar to the breaking of shallow-water waves at beaches. As a consequence, the condition (48) can only be fulfilled for times $t \le T_{\max}$ prior and up to the time $T_{\max}$ at which the breaking occurs.

Upon introducing the abbreviation

$$\alpha = \left(x - t/\sqrt{\epsilon\mu\left(1+3\chi^{(3)}E^2/\epsilon\right)}\right)$$

we have $F(\alpha) = E_0 \exp(-\alpha^2/2\sigma^2)$, so that we may evaluate the condition of the Banach's fix-point theorem (48) for the Gaussian initial condition (47) as

$$\begin{aligned}\sup_{\alpha\in\mathbb{R}}|F'(\alpha)| &= \max_{\alpha\in\mathbb{R}}|F'(\alpha)| \\ &= F'\left(-\frac{E_0}{|E_0|}\sigma\right) = \frac{|E_0|}{\sigma}\exp\left(-\frac{1}{2}\right).\end{aligned} \tag{49}$$

For negative values of the Kerr coefficient $\chi^{(3)} < 0$ and as long as $|3\chi^{(3)}E_0^2/\epsilon| < 1$, we have

$$\max_{|E|\le|E_0|}\left|\frac{\partial\alpha}{\partial E}\right| = \left|\frac{3\chi^{(3)}E_0}{\epsilon}\frac{t}{\sqrt{\epsilon\mu}}\right|\left(1+\frac{3\chi^{(3)}E_0^2}{\epsilon}\right)^{-3/2} \tag{50}$$

As a consequence, we obtain an estimate of the first derivative $F'(E)$ for the Gaussian-pulse initial condition as

$$\left|\frac{\partial F(E)}{\partial E}\right| \le \left|\frac{3\chi^{(3)}E_0^2}{\epsilon}\frac{t}{\sqrt{\epsilon\mu}}\right|\left(\frac{\epsilon+3\chi^{(3)}E_0^2}{\epsilon}\right)^{-3/2}\frac{\exp\left(-\frac{1}{2}\right)}{\sigma}. \tag{51}$$

For sufficiently small values of the time t, this expression is smaller than one so that Banach's fix-point theorem may be applied. This leads to a unique solution of $F(E) = E$ for fixed t and x.

It is now straightforward to employ the implicit function theorem in order to prove that the solution $E(x,t)$ is a continuously differentiable function such that $E(x,t) \in C^1(\mathbb{R}\times[0,T_{\max}])$. In fact, introducing $G(E,x,t) = F(E,x,t) - E$, it follows that $G \in C^1([-|E_0|,|E_0|]\times\mathbb{R}\times[0,T_{\max}])$. The estimate from Banach's fix-point theorem leads to $\partial G(E,x,t)/\partial E = \partial F(E)/\partial E - 1 < 0$, and for the electric field E that results for fixed t and x, we have $G(E,x,t) = 0$. Therefore, if we now proceed to a numerical solution of (46), we are guaranteed that in a neighborhood of each point (E_1,x_1,t_1), there exists a unique $C^1(\mathbb{R}\times[0,T_{\max}])$ function $\tilde{E}(x,t)$, which solves $G(\tilde{E}(x,t),x,t) = 0$. Moreover, these (local) functions $\tilde{E}(x,t)$ exist for all values (x_1,t_1) and the respective neighborhoods overlap, so that, in fact, they represent one and the same function, the unique global solution $E(x,t)$. Therefore, we have determined the reference solution for our exponential integrators of Section II.

In addition, we would like to note that the same calculations regarding existence and uniqueness of solutions can also be carried out for the case of $\chi^{(2)}$ nonlinearities.

In Section III, we compare the performance of several integrators of the nonlinear Maxwell equations (2) for a uniform 1-D system ($\epsilon = 1$, $\mu = 1$, and $\chi^{(3)} = -0.08$) with Gaussian-pulse initial conditions ($E_0 = 1$ and $\sigma = 5/\sqrt{2}$). For this system, we have

$$\left|\frac{\partial F(E)}{\partial E}\right| = \frac{0.24t}{(1-0.24)^{3/2}}\frac{\sqrt{2}}{5}\exp(-0.5) \le 0.0622t. \tag{52}$$

As a result, Banach's fix-point condition (48) is fulfilled for times $t \le 16$ so that we can numerically determine a unique solution of the implicit equation (46) from $t = 0$ to $t = T_{\max} = 16$ and use this as a reference solution. In practice, we solve (46) in the interval $[0, 15]$ with a fix-point iteration scheme up to machine precision (see Section III).

REFERENCES

[1] K. Busch, G. von Freymann, S. Linden, S. F. Mingaleev, L. Tkeshelashvili, and M. Wegener, "Periodic nanostructures for photonics," *Phys. Rep.*, vol. 444, pp. 101–202, 2007.

[2] J. Jin, *The Finite Element Method in Electromagnetics*, 2nd ed. New York: Wiley, 2002.

[3] A. Taflove and S. C. Hagness, *Computational Electrodynamics*. Norwood, MA: Artech House, 2005.

[4] R. M. Joseph and A. Taflove, "Fdtd maxwell's equations models for nonlinear electrodynamics and optics," *IEEE Trans. Antennas Propag.*, vol. 45, no. 3, pp. 364–374, Mar. 1997.

[5] K. Busch, G. Schneider, L. Tkeshelashvili, and H. Uecker, "Justification of the nonlinear schrödinger equation in spatially periodic media," *Z. angew. Math. Phys.*, vol. 57, pp. 905–939, 2006, 11.

[6] R. März, *Integrated Optics: Design and Modeling*. Norwood, MA: Artech House, 1995.
[7] J. Niegemann, L. Tkeshelashvili, and K. Busch, "Higher-order time-domain simulations of maxwell's equations using Krylov-subspace methods," *J. Comput. Theor. Nanosci.*, vol. 4, pp. 627–634, 2007.
[8] B. V. Minchev and W. M. Wright, "A review of exponential integrators for first order semi-linear problems," 2005, vol. 2, pp. 1–44, Tech. Rep. NTNU.
[9] J. D. Jackson, *Classical Electrodynamics*, 1st ed. New York: Wiley, 1975.
[10] M. Fuji and W. J. R. Hoefer, "Multiresolution analysis similar to the FDTD method—Derivation and application," *IEEE Trans. Microw. Theory Tech.*, vol. 46, no. 12, pt. 2, pp. 2463–2475, Dec. 1998.
[11] J. D. Lawson, "Generalized runge-kutta processes for stable systems with large Lipschitz constants," *SIAM J. Numer. Anal.*, vol. 4, no. 3, pp. 372–380, 1967.
[12] C. Moler and C. van Loan, "Nineteen dubious ways to compute the exponential of a matrix, twenty-five years later," *SIAM Rev.*, vol. 45, no. 1, pp. 3–49, 2003.
[13] E. Gallopoulos and Y. Saad, "Efficient solution of parabolic equations by Krylov approximation methods," *SIAM J. Sci. Statist. Comput.*, vol. 13, no. 5, pp. 1236–1264, 1992.
[14] M. Hochbruck and C. Lubich, "On Krylov subspace approximations to the matrix exponential operator," *SIAM J. Numer. Anal.*, vol. 34, no. 5, pp. 1911–1925, 1997.
[15] M. Hochbruck, C. Lubich, and H. Selhofer, "Exponential integrators for large systems of differential equations," *SIAM J. Sci. Comput.*, vol. 19, no. 5, pp. 1552–1574, 1998.
[16] L. Allen and J. H. Eberly, *Optical Resonance and Two-level Atoms*, 2nd ed. New York: Dover, 1987.
[17] J.-G. Ma, "An analytical solution of nonlinear waves propagating in power-law nonlinear dielectric waveguides," *Microw. Opt. Tech. Lett.*, vol. 19, no. 1, pp. 54–57, 1998.
[18] J. D. Begin and M. Cada, "Exact analytical solutions to the nonlinear wave equation for saturable Kerr-like medium: Modes of nonlinear optical waveguides and couplers," *IEEE Trans. Quantum Electron.*, vol. 30, no. 12, pp. 3006–3016, Dec. 1994.
[19] A. S. Desyatnikov and A. I. Maimistov, "Interaction of two spatially separated light beams in a nonlinear kerr medium," *J. Exp. Theor. Phys.*, vol. 86, no. 6, pp. 1101–1106, 1998.
[20] T. Taniuti and K. Nishihara, *Nonlinear Waves*, 1st ed. Boston, MA: Pitman, 1983.

Martin Pototschnig received the Diplom degree in physics and mathematics from the Universität Karlsruhe (TH), Karlsruhe, Germany, in 2006 and 2007, respectively. Currently, he is working towards the Ph.D. degree in physical chemistry at the Swiss Federal Institute of Technology, Zurich, Switzerland.

His research interests include the experimental and theoretical analysis of interaction of two-level systems with electromagnetic radiation.

Jens Niegemann received the Dipl. Phys. degree from the Universität Karlsruhe, Karlsruhe, Germany, in 2004, where he is currently working towards the Ph.D. degree at the Institut für Theoretische Festkörperphysik.

His research interests include numerical methods in electromagnetics and wave propagation in nanostructured materials.

Lasha Tkeshelashvili was born in Tbilisi, Georgia, in 1974. He graduated in physics from Tbilisi State University, Tbilisi, Georgia, in 1996. He received the Ph.D. degree in physics from Karlsruhe University, Karlsruhe, Germany, in 2003.

His research interests include nonlinear phenomena, wave propagation in complex materials, and numerical methods in electromagnetics.

Kurt Busch received the Diplom and Dr. rer. nat degree in physics from the Universität Karlsruhe, Karlsruhe, Germany, in 1993 and 1996, respectively.

After a postdoctoral stay at the University of Toronto, in 2000, he became a Junior Research Group Leader within the Emmy-Noether Program, Deutsche Forschungsgemeinschaft, Universität Karlsruhe. In 2004, he joined the University of Central Florida as an Associate Professor. Since 2005, he has been a Professor of Physics at the Universität Karlsruhe. His research interests lie in the theory of light propagation and light-matter interaction in strongly scattering and nanophotonic systems.

Dr. Busch is the recipient of the 2006 Carl-Zeiss Research Award.